The structure, photochemical reactivity, and photophysical properties of adamantyl X-substituted aryl ethers and a comparison with the alkyl groups, methyl, *tert*-butyl, and allyl[1]

A.L. Pincock and J.A. Pincock

Abstract: The structure, photophysical properties, and photochemistry of the adamantyl aryl ethers **1** in both methanol and cyclohexane have been examined. UV absorption spectra, ^{13}C NMR chemical shifts, X-ray structures, and Gaussian calculations (B3LYP/6-31G(d)) indicate that these ethers adopt a 90° conformer in the ground state. In contrast, fluorescence spectra, excited singlet state lifetimes, and calculations (TDDFT) indicated a 0° conformer is preferred in the first excited singlet state S_1. Irradiation in either solvent results in the formation of adamantane and the corresponding phenol as the major products, both derived from radical intermediates generated by homolytic cleavage of the ether bond. The 4-cyano substituted ether **1j** was the only one to form the ion-derived product, 1-methoxyadamantane (16% yield), on irradiation in methanol. Rate constants of bond cleavage for these ethers from S_1 were estimated by two different methods by comparison with the unreactive anisoles **2**, but the effect of substituents was too small to determine structure–reactivity correlations. The temperature dependence of the quantum yields of the fluorescence of the unsubstituted, 4-methoxy and 4-cyano derivatives of **1** and **2** were also determined. These results indicated that the activated process for **1** was mainly bond cleavage for the 4-cyano substrate whereas for **2**, it was internal conversion and intersystem crossing.

Key words: aryl ether photochemistry, fluorescence, excited-state rate constants, excited-state temperature effects.

Résumé : On a étudié la structure, les propriétés photophysiques et la photochimie des oxydes d'adamantyle et d'aryles **1**, tant dans le méthanol que dans le cyclohexane. Les spectres d'absorption UV, les déplacements chimiques en RMN du ^{13}C, les structures obtenues par diffraction des rayons X et les calculs gaussiens (B3LPYP/6-31G(d)) indiquent que dans leur état fondement ces éthers adoptent un conformère à 90°. Par opposition, les spectres de fluorescence, les temps de vie de l'état singulet excité et les calculs (TDDFT) indiquent qu'un conformère à 0° est privilégié dans le premier état singulet excité, S_1. Les produits principaux d'une irradiation dans l'un ou l'autre des solvants sont l'adamantane et le phénol correspondant qui dérivent tous les deux d'intermédiaires radicalaires générés par un clivage homolytique de la liaison éther. L'irradiation dans le méthanol du dérivé **1j** portant un substituant 4-cyano est le seul à conduire à la formation du 1-méthoxyadamantane (rendement de 16 %), le produit dérivé de l'ion. On a utilisé deux méthodes différentes pour évaluer les constantes de vitesse de clivage de la liaison de ces éthers à partir de S_1 par comparaison avec des anisoles non réactifs (**2**); l'effet des substituants est toutefois trop faible pour déterminer des corrélations structure–activité. On a aussi établi la relation entre la température et le rendement quantique de fluorescence des dérivés des composés **1** et **2**, non substitués ou portant des substituants 4-méthoxy ou 4-cyano. Ces résultats indiquent que le processus activé pour le composé **1** est le clivage de la liaison pour le substrat 4-cyano alors que pour le composé **2** il s'agit de la conversion interne et d'un passage intersystème.

Mots clés : photochimie d'éthers aromatiques, fluorescence, constantes de vitesse d'états excités, effets de température sur l'état excité.

[Traduit par la Rédaction]

Introduction

The effect that substituents (X) on aromatic rings (Ar) have on the quantum yields and rate constants of bond cleavage reactions from photochemically generated excited singlet states of substrates of the general class ArY–Z, where the Y—Z bond is the reactive one, continue to attract interest. The objective is to develop excited state structure–reactivity relationships, like the Hammett equation, that are well-established for ground-state reactions. Related to this

Received 9 December 2004. Published on the NRC Research Press Web site at http://canjchem.nrc.ca on 12 October 2005.

A.L. Pincock and J.A. Pincock.[2] Department of Chemistry, Dalhousie University, Halifax, NS B3H 4J3, Canada.

[1]This article is part of a Special Issue dedicated to organic reaction mechanisms.
[2]Corresponding author (e-mail: james.pincock@dal.ca).

 doi: 10.1139/V05-117

Scheme 1. Mechanism and products formed from the homolytic cleavage of alkyl aryl ethers and rate constants of reaction for S_1.

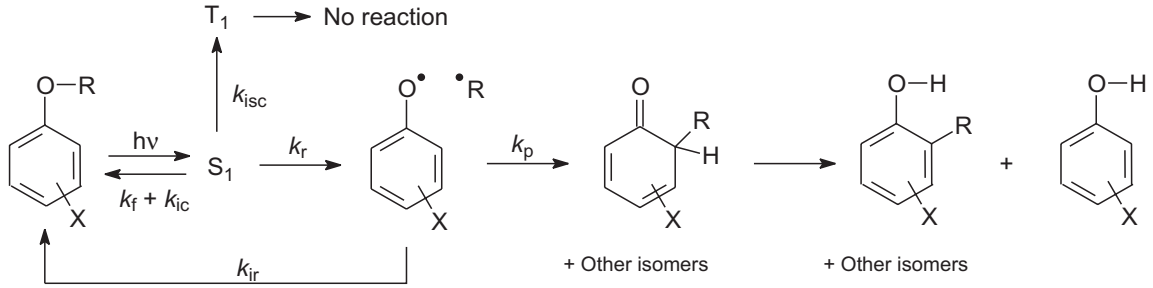

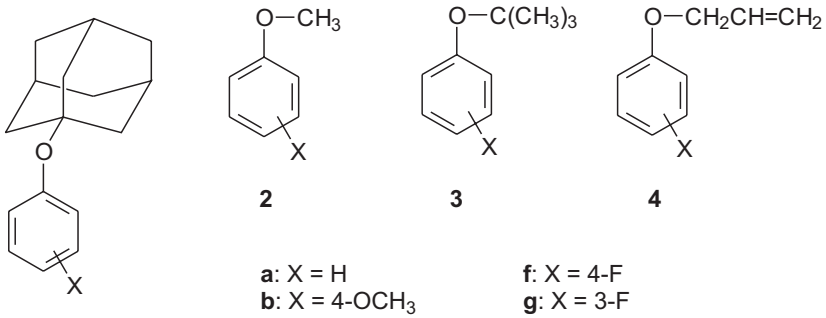

a: X = H
b: X = 4-OCH_3
c: X = 3-OCH_3
d: X = 4-CH_3
e: X = 3-CH_3
f: X = 4-F
g: X = 3-F
h: X = 4-CF_3
i: X = 3-CF_3
j: X = 4-CN
k: X = 3-CN

goal has been one of understanding, in the excited-state cases, the competition between the formation of the products derived from radical pairs (from homolytic cleavage of the Y—Z bond) and ion pairs (from heterolytic cleavage of the Y—Z or from rapid, exergonic redox electron transfer in the first formed radical pair). A general review of the mechanistic principles involved and a survey of the observed reactivity of the Z groups for arylmethyl cases (Y = CH_2) have been published (1).

We now summarize results for four series of the class of compounds ArO-C (**1**–**4**), i.e., phenolic ethers where Y = O and Z = C. New results will be given for the adamantyl aryl ethers **1**, in comparison with the anisoles **2**. Previously, we have reported on the photochemistry and photophysics of the *tert*-butyl (**3**) (2) and allyl ethers (**4**) (3). For these latter two cases, the products of photolysis in either methanol or cyclohexane were, in general, those expected from homolytic cleavage of the carbon–oxygen bond to form a radical pair followed by in-cage coupling (photo-Fries for **3**, photo-Claisen for **4**) or disproportionation (Scheme 1). For both, the reactions were shown to occur from the excited singlet state (S_1) by selective triplet quenching studies.

Rate constants k_r for the reaction from the excited singlet state for the *tert*-butyl compounds **3** were determined by the classic quantum yield (Φ_r) of the reaction method (eq. [1]) (2). The rate constants for S_1 of the reaction (k_r), fluorescence (k_f), internal conversion (k_{ic}), and intersystem crossing (k_{isc}) are shown in Scheme 1. The sum of these is k_t, the reciprocal of τ_s, the excited singlet state lifetime. Measurement of Φ_r by the disappearance of starting material and τ_s by fluorescence decay gives k_r. The rate constants obtained in this way gave a reasonable correlation with $\sigma^{h\nu}$ (4) and $\rho = -0.77$ ($r = 0.975$) for seven of the 10 compounds of set **3** studied where $\sigma^{h\nu}$ values were available. This correlation was surprising because the $\sigma^{h\nu}$ scale was developed from results for the photoprotonation of styrenes and phenylacetylenes, reactions that result in positive charge increases at the benzylic carbon in the rate-determining transition state, **5** for styrenes. A similar transition state (**6**) for the photo-Fries reaction of the *tert*-butyl ethers **3** seems less likely than one of opposite polarity (**7**). However, a very poor (nonexistent) correlation of the rate constants for **3** with the values of σ^{ex} (5–7), which are derived from the excited state pK_as of phenols **8**, was obtained.

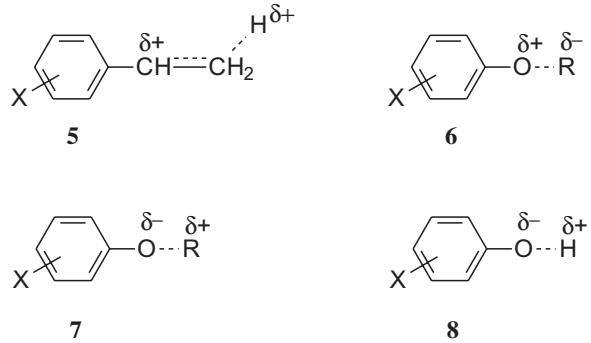

$$[1] \qquad \Phi_r = \frac{k_r}{k_f + k_{ic} + k_{isc} + k_r} = \frac{k_r}{k_t} = k_r \tau_s$$

While studying the *tert*-butyl ethers **3** (2), we also examined the 4-cyano compound **1j** from the adamantyl derivatives. An interesting result was that on photolysis of **1j** in methanol, the ion-derived product 1-methoxyadamantane was obtained in 16% yield. This compound was synthesized

Scheme 2. Products of the photolysis of adamantyl ethers **1** in methanol and cyclohexane.

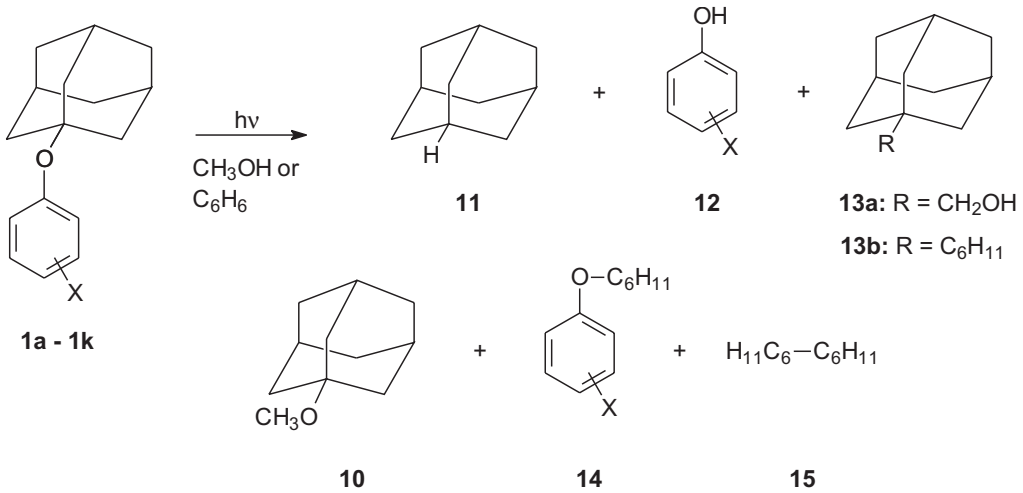

by reaction of the lithium salt of 1-adamantanol with 4-fluorobenzonitrile (8), a nucleophilic aromatic substitution reaction that relies on the electron-withdrawing nitrile group in the para position. This procedure was unsuccessful for 3-fluorobenzonitrile. Therefore, the other substituted derivatives of **1** were not previously studied.

We now report on the synthesis, photochemistry, photophysical properties, and excited-state rate constants for the complete set of the adamantyl ethers **1**. These compounds have an advantage that the fate of the non-aryl fragment of the ether cleavage reaction can be easily observed. This was not so for the very volatile fragments ($CH_3OC(CH_3)_3$, $CH_3OCH_2CH{=}CH_2$, etc.) expected from sets **3** and **4**.

Results and discussion

Synthesis of 1-adamantyl aryl ethers (1a–1k)

The ethers were synthesized by reaction of 1-bromoadamantane (by heating in pyridine) with the corresponding substituted phenols according to a method described previously (9) (eq. [2]). The reaction mixtures were not homogeneous. The reactions were usually monitored by GC-FID until the 1-bromoadamantane (the limiting reagent) had disappeared. The crude product always contained varying amounts of the isomeric (GC–MS) 1-adamantylphenol derivatives **9**, which were not characterized. However, because these isomers were possible products in the photochemistry of the ethers **1**, their GC retention times were useful. They could easily be removed by flash chromatography on silica gel and the ethers purified by crystallization. The yields after purification ranged from 20% to 35%. Characterization data are given in the Experimental section; ^{13}C NMR data, along with those of sets **2**, **3**, and **4**, which will be discussed in the following, are given in Table S1 (Supporting information).[3]

Photochemistry of 1-adamantyl aryl ethers 4a–4k in methanol and cyclohexane

The ethers **1** were photolyzed in either methanol or cyclohexane with 254 nm lamps in a Rayonet reactor at 25 °C. The reactions were reasonably efficient with little dependence on the substituent. For instance, for approximately 100 mg samples, 83% of the unsubstituted compound **1a** and 80% of the 4-methoxy compound **1b** in 100 mL of methanol had reacted after 30 min. The reactions were a factor of two to three times slower in cyclohexane. In both solvents in all cases, except for the 4-cyano compound **1j** in methanol, the products were those expected from the formation of radicals by homolytic cleavage of the C—O bond (Scheme 2). As reported previously (2), 16% of the methyl ether **10** was formed from **1j** in methanol indicating a minor intervention of a pathway involving ion pairs. In agreement with this observation, 4-cyanophenoxide has been used as a leaving group for the generation of diphenylmethyl cations (observable by nanosecond LFP) from diphenylmethyl ethers (10),

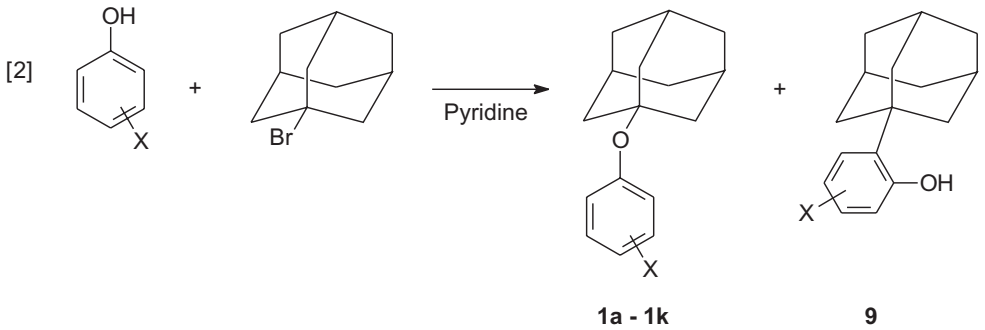

[3] Supplementary data for this article are available on the Web site or may be purchased from the Depository of Unpublished Data, Document Delivery, CISTI, National Research Council Canada, Ottawa, ON K1A 0S2, Canada. DUD 4020.

and in the pioneering study by Zimmerman and Somasekhara (11) on photochemically generated triphenylmethyl cations.

The major product from the adamantyl fragment of the ethers **1** for all substrates in both solvents was adamantane **11**, derived from the 1-adamantyl radical and accounting for 70%–90% of the mass balance. This is reasonable on the basis of the fact that hydrogen atom abstraction by the 1-adamantyl radical from both methanol and cyclohexane is somewhat more favourable than by the *tert*-butyl radical (C–H BDE = 99, 96, 99, and 96 kcal/mol for 1-adamantane, methanol, cyclohexane, and 2-methylpropane, respectively) (1 cal = 4.184 J) (12). The major product from the aryl fragment was the corresponding phenol **12**, but these gave very broad and tailing peaks in the GC traces that could not be reliably quantified. Photo-Fries products (GC–MS, 15% yield overall, presumably 2- and 4-(1-adamantyl)phenol) were only observed for **1a** in methanol. Low yields of products **13a**, **13b**, **14**, and **15** (Scheme 2) were also formed from the solvent-derived radicals.

Geometry of aryl ethers 1–4 in the ground state

The geometry and rotational barriers for the methoxy group of anisole have been extensively studied by both experimental and computational methods. Two limiting structures have been considered: **16** with a $C(H_3)$-O-C1-C2 dihedral angle of $\Phi = 0°$ and **17** with the same angle equal to 90°. For **16**, an sp^2 hybridization model predicts conjugative overlap between the oxygen centered lone pair in a π orbital and the π system of the aromatic ring as indicated by the resonance structures **16a** and **16b**. For **17**, either an sp^2 or sp^3 hybridization model predicts a weaker interaction. Clearly, a vast body of experimental evidence demonstrates that the methoxy group in anisole is a π donor and therefore **16** must be the minimum energy structure on the rotational surface. A more difficult question to answer is the position of **17** on this surface.

Most experimental studies have indicated a twofold rotational surface with **17** as a maximum at ~4 kcal/mol above **16** (13). Therefore, rotation between the two minima ($\Phi = 0°$ and 180°) would be rapid on the NMR timescale at room temperature. However, long-range C–H NMR coupling constants demonstrate that **17** is in a shallow minimum and therefore the rotational surface is fourfold (14). Calculations by ab initio methods have located this minimum with some basis sets but not with others (13). For instance, at the RHF/6-31G* level, **17** is 1.39 kcal/mol above **16**, and the transition state between the two (Φ = ~65°) is 1.59 kcal/mol above **16**. These same calculations give C-O-C1 bond angles of 119.8° and 115.5° for **16** and **17**, respectively. A conformational minimum similar to **16** has been found for allyl phenyl ether (**4a**: X–H) (15).

In terms of the photochemical reactivity of ethers **1**, **3**, and **4** (as discussed later, the anisoles are photochemically unreactive), **16** has the reactive C—O bond perpendicular to the π system of the aromatic chromophore whereas **17** has the same C—O bond parallel to it. Therefore, **17** should be more reactive. As discussed now, we have used a variety of probes to assess the conformational geometry of aryl ethers in the ground state and conclude that the tertiary alkyl derivatives **1** and **3**, in contrast to the anisoles **2** and the allyl ethers **4**, have preferred geometries analogous to **17**.

UV absorption spectra of ethers 1–4 in methanol and cyclohexane

The long wavelength absorption band λ_{max} (L_b transition) and molar absorptivity (ϵ) for the 1-adamantyl ethers **1a**–**1k**, and for comparison, the corresponding anisoles **2a**–**2k** in both methanol and cyclohexane as the solvent are reported in Table 1. Values for the *tert*-butyl ethers **3a**–**3i** in methanol and **3a**–**3c** in cyclohexane are also included. The L_b band for the anisoles has a significantly higher ϵ, and the λ_{max} tends to occur at longer wavelengths than the tertiary alkyl cases **1** and **3**. These trends are shown graphically in Fig. 1 for X = H, 4-OCH_3, and CN[4] in both methanol (left in each case) and cyclohexane (right in each case). The spectra for the corresponding allyl derivatives, which have been reported previously (3), are also included in these figures. The spectra for X = 4-CN and 4-CF_3 are not typical of those for the other substituents because these electron-withdrawing groups interact strongly with the ether oxygen and shift the L_a band to longer wavelengths, partially obscuring the L_b band. The primary ethers (allyl (**4**) and methyl (**2**)) have very similar spectra that differ significantly (higher ϵ values, longer wavelengths) from those of the tertiary alkyl ethers **1** and **3**.

Similar observations have been made previously for anisoles that are sterically crowded by ortho substitution at C-2 and C-6 (16). For instance, the λ_{max} of the L_b band in

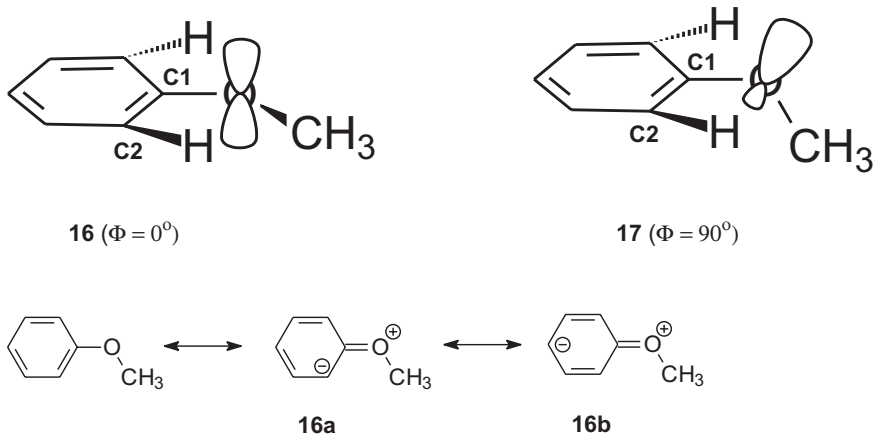

[4] These three were chosen to span the complete range of electron-donating and electron-withdrawing abilities of all the substituents studied.

Table 1. Absorbance and fluorescence data and excited-state rate constants for ethers **1–3** in methanol and cyclohexane.

	X	Solvent[a]	λ_{max}[b] (nm)	ϵ[b] ((mol/L)$^{-1}$ cm^{-1})	$\lambda_{0,0}$[c] (nm)	$E(S_1)$ (kJ/mol)	Φ_f[e]	τ^{sf} (ns)	k_t ($10^7 s^{-1}$)	k_f(exp) ($10^7 s^{-1}$)	k_f (calcd) ($10^7 s^{-1}$)	k_f(exp)/k_f (calcd)[g]	$k_t^M - k_t$ ($10^7 s^{-1}$)
1a	H	M	256	328	280	427	0.23	6.21	16.1	3.7	0.9	3.97	2.9
2a	H	M	271	1680	281	427	0.24[h]	7.58	13.2	3.2	2.4	1.33	
3a	H	M	269	519									
1a	H	C	270	505	279	431	0.21	7.00	14.3	3.0	1.1	2.63	1.5
2a	H	C	271	1930	281	427	0.29[i]	7.80	12.8	3.7	3.6	1.03	
3a	H	C	269	574									
1b	4-OCH_3	M	280	1894	299	402	0.085	2.50	40.0	3.4	2.7	1.24	2.7
2b	4-OCH_3	M	290	2820	305	393	0.11	2.68	37.3	4.1	4.3	0.93	
3b	4-OCH_3	M	280	2000									
1b	4-OCH_3	C	282	2190	298	402	0.090	3.12	32.0	2.6	3.6	0.72	–1.1
2b	4-OCH_3	C	289	3200	304	383	0.12	3.02	33.1	4.0	5.5	0.71	
3b	4-OCH_3	C	280	2140									
1c	3-OCH_3	M	272	1930	281	427	0.084	2.54	39.3	3.8	2.9	1.32	–2.0
2c	3-OCH_3	M	274	2200	285	419	0.076	2.42	41.3	3.1	3.1	1.00	
3c	3-OCH_3	M	272	1723									
1c	3-OCH_3	C	272	1910	283	423	0.106	2.63	38.0	4.0	3.0	1.32	–2.3
2c	3-OCH_3	C	274	2220	284	423	0.093	2.48	40.3	3.7	3.5	1.09	
3c	3-OCH_3	C	272	1777									
1d	4-CH_3	M	269	649	288	414	0.162	5.91	16.9	4.4	1.0	4.36	1.2
2d	4-CH_3	M	279	1880	289	414	0.22	6.37	15.7	3.5	3.1	1.12	
1d	4-CH_3	C	270	759	288	414	0.226	6.62	15.1	3.4	1.3	2.58	1.8
2d	4-CH_3	C	279	2170	290	414	0.33	7.48	13.3	4.4	3.9	1.13	
1e	3-CH_3	M	266	452	283	423	0.17	6.90	14.4	2.4	0.8	3.08	2.0
2e	3-CH_3	M	273	1660	283	423	0.27	8.0	12.4	3.4	2.8	1.21	
1e	3-CH_3	C	266	486	283	423	0.23	7.69	13.0	3.0	0.9	3.26	1.7
2e	3-CH_3	C	273	1810	282	423	0.37	8.79	11.3	4.2	3.4	1.24	
1f	4-F	M	264	1240	284	423	0.14	3.44	29.1	4.0	1.9	2.13	2.2
2f	4-F	M	280	2670	291	410	0.15	3.72	26.9	4.0	4.1	0.98	
3f	4-F	M	269	1200									
1f	4-F	C	271	1550	289	414	0.14	3.54	29.2	4.0	2.6	1.56	3.3
2f	4-F	C	281	2900	290	414	0.18	3.86	25.9	4.0	4.9	0.94	
1g	3-F	M	263	1344	277	431	0.0047	—	—	—	1.9	—	
2g	3-F	M	269	1590	279	431	0.0055	—	—	—	2.3	—	
3g	3-F	M	263	947									
1g	3-F	C	263	905	276	435	0.014	—	—	—	1.7	—	
2g	3-F	C	269	1650	278	431	0.022	0.8	125.0	—	2.9	1.0	
1h	4-CF_3	M	260	434	282	423	0.073	3.76	26.5	1.9	—	—	4.1
2h	4-CF_3	M	270	1060	279	431	0.093	4.47	22.4	2.1	—	—	
3h	4-CF_3	M	260	551									
1h	4-CF_3	C	262	433	281	427	0.10	4.35	22.9	2.3	—	—	3.1
2h	4-CF_3	C	270	1100	280	427	0.13	5.05	19.8	2.6	—	—	
1i	3-CF_3	M	267	1180	289	414	0.037	2.90	34.4	1.3	2.0	0.65	2.8
2i	3-CF_3	M	277	2310	288	414	0.11	3.16	31.6	3.5	3.7	0.95	
3i	3-CF_3	M	273	1163									
1i	3-CF_3	C	268	1290	288	414	0.056	3.17	31.5	1.8	2.5	0.72	2.2
2i	3-CF_3	C	267	2440	289	414	0.16	3.41	29.3	3.2	4.4	0.73	
1j	4-CN	M	274 (sh)	1230	286	419	0.051	2.30	43.5	2.2	—	—	13.9
2j	4-CN	M	271 (sh)	2030	286	419	0.075	3.37	29.6	2.2	—	—	
1j	4-CN	C	267 (sh)	1150	287	419	0.083	4.41	22.6	1.9	—	—	5.6
2j	4-CN	C	274	1310	286	419	0.11	5.88	17.0	1.9	—	—	
1k	3-CN	M	286	1440	305	393	0.094	2.97	33.6	3.1	2.2	1.41	7.5

Table 1 (*concluded*).

	X	Solvent[a]	λ_{max}[b] (nm)	ϵ[b] ((mol/L)$^{-1}$ cm^{-1})	$\lambda_{0,0}$[c] (nm)	$E(S_1)$ (kJ/mol)	Φ_f[e]	τ[sf] (ns)	k_t ($10^7 s^{-1}$)	k_f(exp) ($10^7 s^{-1}$)	k_f (calcd) ($10^7 s^{-1}$)	k_f(exp)/k_f (calcd)[g]	$k_t^M - k_t$ ($10^7 s^{-1}$)
2k	3-CN	M	290	2960	305	393	0.14	3.60	27.7	3.9	4.5	0.87	
1k	3-CN	C	286	1400	300	398	0.14	4.09	24.4	3.5	2.4	1.46	3.7
2k	3-CN	C	288	2980	300	398	0.20	4.83	20.7	4.1	5.1	0.80	

[a]M is methanol, C is cyclohexane.
[b]Obtained from absorption spectra.
[c]Obtained from the overlap of the absorption and fluorescence spectra.
[d]Calculated from $E_{S_1} = 12.0 \times 10^4/\lambda_{0,0}$.
[e]Quantum yield of fluorescence relative to anisole in methanol (0.24) and cyclohexane (0.29), estimated error ±10%.
[f]Singlet lifetime by nanosecond single photon counting. The standard deviations of the fits to the experimental counts are <2%. No value indicates that the lifetime was less than 0.5 ns.
[g]The values of k_f(calcd) could not be obtained for X = 4-CF_3 and 4-CN because the L_a band was at a long enough wavelength so as to obscure the short wavelength portion of the L_b band, preventing the use of eq. [5].
[h]G. Kohler, G. Kittel, and N. Getoff. J. Photochem. **18**, 19 (1985).
[i]I.B. Berlman. Handbook of fluorescence spectra of aromatic molecules. Academic Press, New York. 1971. p. 139.

2,6-dimethylanisole shifts to shorter wavelengths (266 nm) and lower molar absorptivity (620 (mol/L)$^{-1}$ cm^{-1}) compared to anisole itself (269 nm, 2100 (mol/L)$^{-1}$ cm^{-1} (16); 271 nm, 1980 (mol/L)$^{-1}$ cm^{-1} (Table 1),[3] both in cyclohexane). The proposed explanation is that ortho substitution forces the methoxy group into the 90° geometry of **17**, reducing the importance of structures **16a** and **16b** that allow conjugation of the oxygen lone pair with the aryl ring.

^{13}C NMR spectra of ethers 1–4 in $CDCl_3$

Complete ^{13}C NMR spectral data for the adamantyl ethers **1** along with those for the anisoles **2**, *tert*-butyl ethers **3**, and the allyl ethers **4**, are given in Table S1 (Supporting information).[3] The anisole data were taken from the Aldrich compilation (17) and these values were confirmed for the para-substituted compounds by another literature source (18). The allyl ether data, which differ insignificantly from the anisole data, have been reported previously (3). Relative to the anisole derivatives, the ^{13}C chemical shifts at C-4 for both the adamantyl and *tert*-butyl derivatives have higher δ values (deshielded) by an average of 2.57 ± 0.52 ppm (11 compounds) and 2.97 ± 0.38 (nine compounds), respectively. Moreover, these changes vary around these averages in a random way over the range of X groups from electron-donating ones (CH_3O, CH_3) to electron-withdrawing ones (CF_3, CN) in either the meta or para position. Therefore, the contribution that resonance structure **16b** makes is not more important for a resonance electron-withdrawing group like CN.

For ortho-substituted anisoles, the same effect has been observed previously (19) with changes in ^{13}C δ values at C-4 relative to anisole of –0.3 ppm (2-methyl), +3.9 ppm (2,6-dimethyl), +7.2 ppm (2,6-diisopropyl), and +9.7 ppm (2,6-di-*tert*-butyl). These deshielding effects are a consequence of the lowering of the π-electron density at C-4 and reflect the decreasing importance of the resonance contributor **16b** as conformation **17** becomes more dominant. Therefore, the bulky *tert*-butyl and 1-adamantyl alkyl groups are providing a similar steric inhibition to a resonance interaction of the ether oxygen with the benzene ring as the case for two ortho methyl groups on the benzene ring. The effect that these bulky groups have at C-2 and C-6 is even larger (changes in δ values ranging from –10.5 to –11.5 ppm for the adamantyl ethers relative to the anisoles), but these changes probably reflect to some extent a direct steric interaction rather than only the importance of resonance effects.

Molecular orbital calculations

Two views of each of the two stable conformers for 1-adamantyl phenyl ether (**1a**: X = H) are shown in Figs. 2 and 3, the former corresponding to the 0° structure **16** and the latter to the 90° structure **17**. These were obtained as geometry optimized minima by GAUSSIAN 98 (20) at the B3LYP/6-31G(d) level of theory.[5] Similar calculations were performed for the para-substituted cases shown in Table 2 with OH replacing OCH_3 for computational convenience. Frequency analyses indicated that all were minima with all frequencies positive except for small negative values corresponding to methyl rotations for X = CH_3. The lowest energy positive frequencies (~35 cm^{-1} for **16** and ~15 cm^{-1} for **17**) correspond, by visualization in GaussView, to the rotation interconverting **16** and **17**.

After correction for zero point energy, the 90° conformer is calculated to be the more stable for all cases although the difference in energy between the two decreases systematically as the substituent changes from the resonance electron-donating 4-hydroxy group to the electron-withdrawing 4-cyano group. Clearly, this difference is dominated by the steric preference for the 90° geometry, which moves the ortho hydrogens on the benzene ring away from the adamantyl hydrogens. This steric crowding in the 0° structure is indicated by the large calculated O-C1(aryl)-C2(aryl) and C1(adamantyl)-O-C1(aryl) bond angles of 127.5° and 126.8°, respectively, at the ether functional group in contrast to 120.1° and 102.7° for the corresponding angles in the 90° structure. The energetic preference for the 90° conformer is decreased by conjugation of the oxygen lone pair of the ether with the substituent so that the 0° and 90° conformers are calculated to have almost identical stabilities for X = 4-CN. A related observation has been made previously for diphenyl ethers, monosubstituted on one of the two rings (21). The more stable conformer changes from that ring hav-

[5]The optimized geometries in C_1 symmetry have actual dihedral angles of 0.1° for the "0°" structure and 92.7° for the "90°" structure.

Fig. 1. UV absorption spectra of the ethers **1–4** for X = H, 4-OCH_3, and 4-CN in methanol (right) and cyclohexane (left).

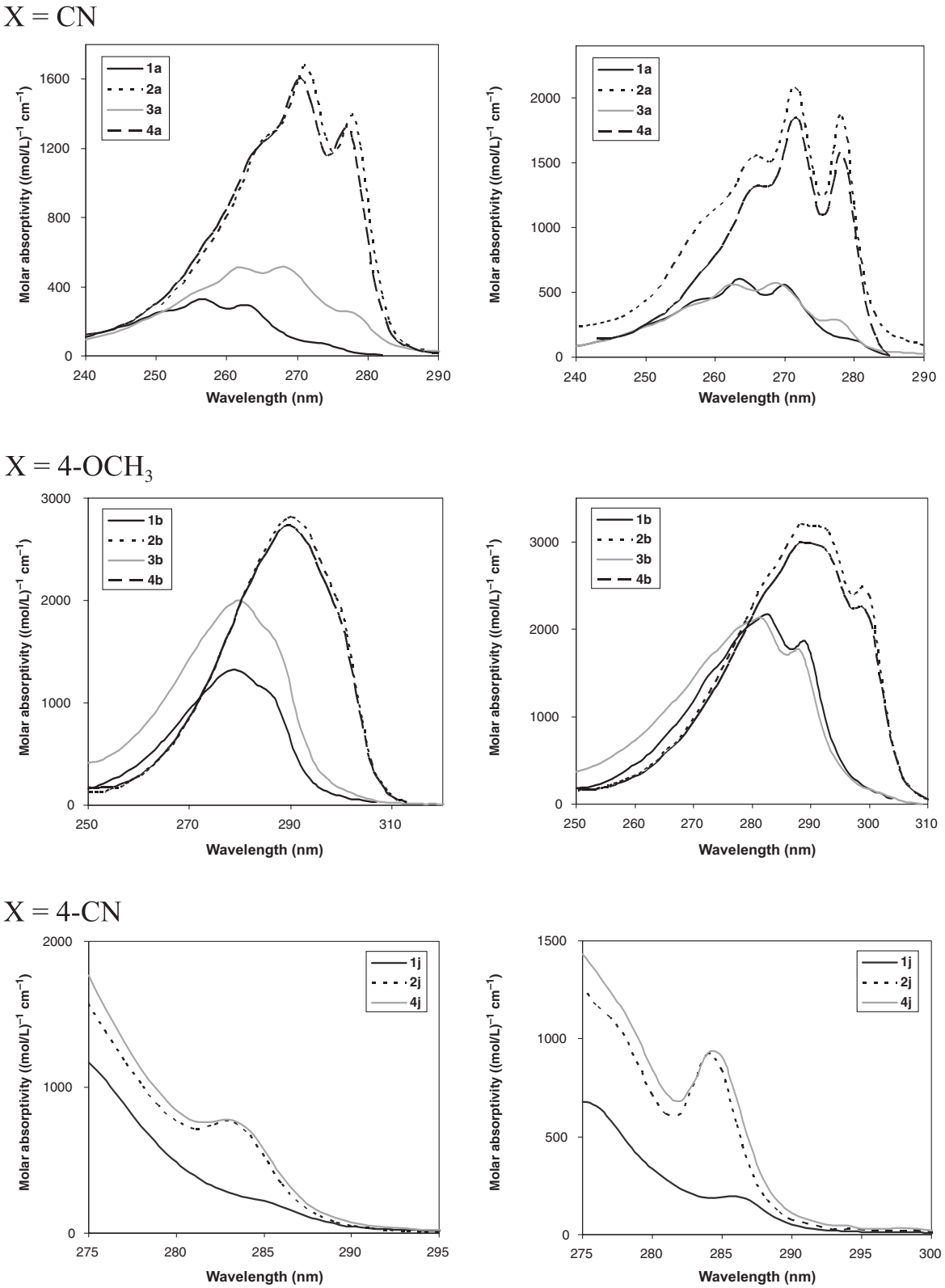

ing conjugation to the ether oxygen for 4-CN (0°) to that conjugation being reduced for 4-OH (90°).

A scan of the dihedral angle from –105° to 105° (optimizing all other variables) for the unsubstituted case **1a** gives the energy surface shown in Fig. 4. A very shallow minimum is observed at the 0° geometry with a barrier of approximately 0.2 kJ/mol that separates it from the two identical minima at ±92°. This plot is quite similar to that

Table 2. Calculated (GAUSSIAN 98) values for aryl adamantyl ethers **1** at the two minimum energy conformers.

4-X	Dihedral angle (°)	E(SCF)[a] (Hartree)	ΔE[b] (kJ/mol)	E(SCF + ZPE)[c] (Hartree)	ΔE(ZPE)[b] (kJ/mol)	E(Ex)[d] (kJ/mol)	Osc. strength	$\Delta E(S_1)$[b] (kJ/mol)
OH	0	–772.19879		–771.86533		535.8	0.083	–8.0
OH	90	–772.20166	–7.5	–771.86863	–8.7	552.5	0.059	
F	0	–796.21732		–795.89594		552.5	0.069	–10.8
F	90	–796.21948	–5.7	–795.89863	–7.1	570.1	0.039	
CH_3	0	–736.30263		–735.94560		552.5	0.053	–8.4
CH_3	90	–736.30448	–4.8	–735.94797	–6.2	567.0	0.016	
H	0	–696.98521		–696.65781		565.4	0.035	–6.3
H	90	–696.98691	–4.5	–696.65781	–6.1	577.4	0.009	
CN	0	–789.23183	–1.1	–788.90365		536.3	0.287	–2.1
CN	90	–789.23141		–788.90378	–0.4	539.4	0.234	

[a]Calculated at optimized geometries by B3LYP/6-31G(d).
[b]The negative values indicate the more stable structure of the pair for each X substituent.
[c]After zero point energy correction at optimized geometry.
[d]Calculated by TDDFT/6-31G(d) at the optimized ground-state geometry.

Fig. 2. Two views of the B3LYP/6-31G(d) optimized geometry with a C1(adamantyl)-O-C1(aryl)-C2(aryl) dihedral angle of 0.1°. The O-C1(aryl)-C2(aryl) and the C1(adamantyl)-O-C1(aryl) bond angles are 127.5° and 126.6°, respectively.

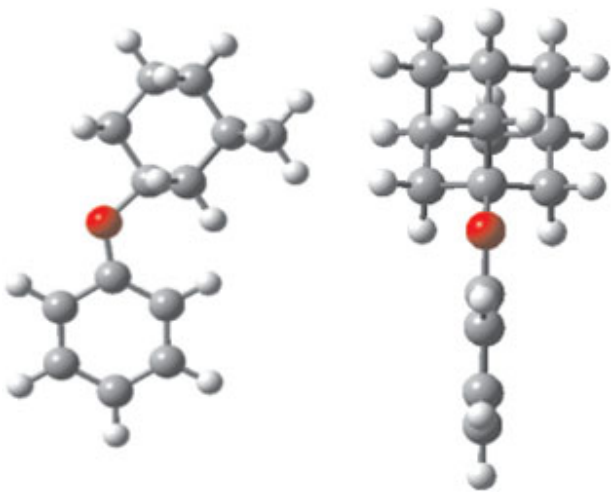

Fig. 3. Two views of the B3LYP/6-31G(d) optimized geometry with a C1(adamantyl)-O-C1(aryl)-C2(aryl) dihedral angle of 92.7°. The O-C1(aryl)-C2(aryl) and the C1(adamantyl)-O-C1(aryl) bond angles are 120.1° and 102.7°, respectively.

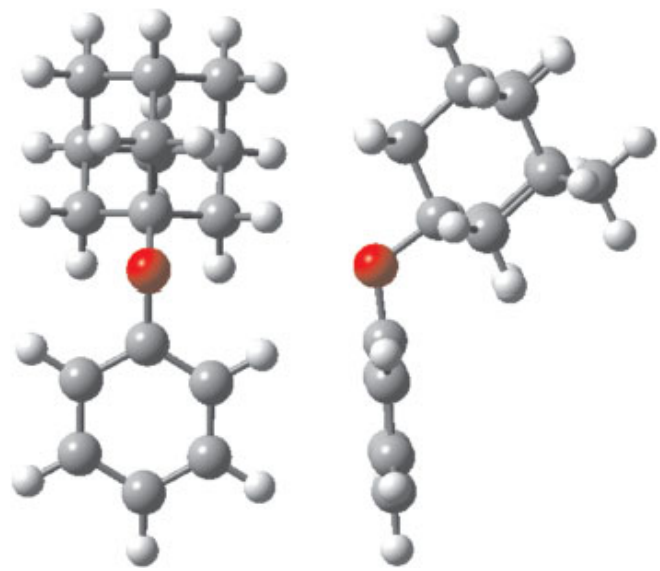

calculated for anisole with the contrast that the minimum energy conformation (90° for **1** and 0° for anisole) is complimentary for the two cases.

X-ray structures of adamantyl ethers 1b (X = 4-OCH$_3$) and 1h (X = 4-CF$_3$)

Suitable crystals were obtained for X-ray crystallograph structures[6] for these two compounds and that for **1b** is shown in Fig. 5. In both cases, a geometry similar to the 90° structure is preferred; the observed dihedral angles are 99° for **1b** and 107° for **1h**. These derivations from the symmetrical 90° structures are likely due to intermolecular crystal packing forces.

Geometry of the aryl ethers 1–4 in the excited singlet state

Information about the geometry of aryl ethers in the excited state can be obtained from fluorescence measurements using both excited singlet state lifetimes and steady-state spectra, and MO calculations. The conclusion is that the 0° structure is energetically preferred for S_1.

Excited singlet state lifetimes of ethers 1 and 2

The total rate of decay ($k_t = 1/\tau_s$) of the excited singlet state (τ_s from nanosecond single photon counting) along with the fluorescence quantum yields are reported in Table 1 in both methanol and cyclohexane solvents for the adamantyl **1** and methyl ethers **2**. The rate constants of fluorescence ($k_f = \Phi_f k_t$) are also given. Averaged over all substituted compounds, the ratios of $k_f(\mathbf{2})/k_f(\mathbf{1}) = 1.19 \pm 0.35$ and 1.26 ± 0.24 (10 compounds) in methanol and cyclohexane, respectively, are equal to unity, within experimental error. In fact, these ratios are improved to 1.02 ± 0.15 and $1.20 \pm$

[6]T.S. Cameron. Department of Chemistry, Dalhousie University. Unpublished results. 2004.

Fig. 4. Relative energy vs. the C1(adamantyl)-O-C1(aryl)-C2(aryl) dihedral angle for adamantyl phenyl ether by B3LYP/6-31G(d).

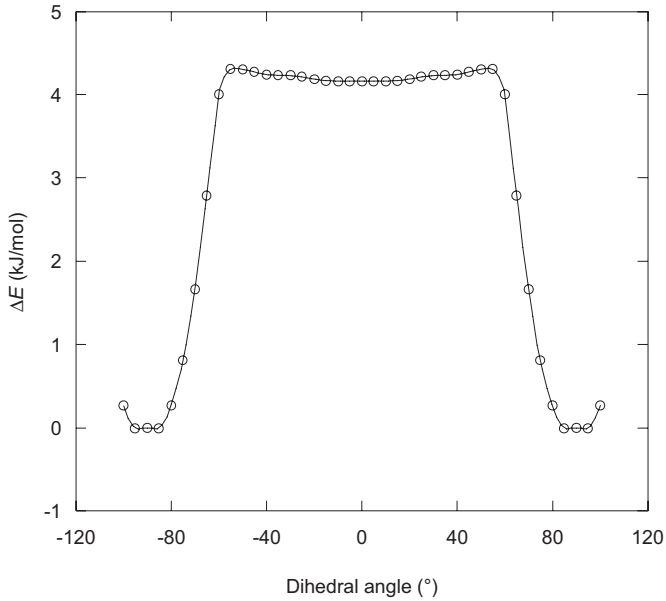

0.23, respectively, if the values for X = 3-CF_3, which seem unusually large, are not included in the two averages.

The general theoretical relationship (22, 23) between the radiative lifetime ($\tau_f = 1/k_f$) and the absorbance spectrum is given in eq. [3] where n is the refractive index of the solvent, υ_f is the expectation value for the frequency of the fluorescence spectrum, and the final term is the integrated absorbance spectrum. The constant gives k_f in units of s^{-1} if the frequency values are expressed in wavenumber (cm^{-1}), and molar absorptivity ϵ in the usual units ($(mol/L)^{-1}$ cm^{-1}). This equation is derived on the basis of the oscillator strength model and the important assumption that the excited singlet state and the ground state have similar geometries. It has been used successfully in the past for simple aromatic compounds like benzene, toluene, and *ortho*-xylene (24), and by us for the anisoles **2** and the allyl ethers **4** (3).

$$[3] \qquad k_f = 2.88 \times 10^{-9} n^2 < \bar{\nu}_f > \int \epsilon \ln \bar{\nu}$$

Equation [3] works very well for the anisoles **2** in both methanol and cyclohexane, k_f(exp)/k_f(calcd) = 1.05 ± 0.10 (seven compounds) and k_f(exp)/k_f(calcd) = 0.96 ± 0.13 (10 compounds), respectively. These values are in Table 1.

In contrast, as shown in Table 1, eq. [3] does not work as well for the adamantyl ethers **1**, with k_f(exp)/k_f(calcd) = 2.27 ± 1.14 (eight compounds) and k_f(exp)/k_f(calcd) = 1.98 ± 0.83 (eight compounds) in methanol and cyclohexane, respectively. The larger scatter and the average significantly greater than unity is a consequence of the decreases in ϵ for the adamantyl ethers. In general, the lower ϵ values decrease k_f(calcd) values and consequently increase ratios of k_f(exp)/k_f(calcd). As discussed above, these lower values of ϵ for the adamantyl ethers **1** were ascribed to these ethers preferring the 90° geometry rather than the 0° geometry.

The similarity in the experimental k_f values for the anisoles **2** and the adamantyl ethers **1** suggest similar excited-state geometries for both. The good agreement among the k_f values obtained experimentally and from eq. [3] for the anisoles indicates that the ground-state and excited-state geometries are similar, presumably the 0° structure **16**. In contrast, for the adamantyl ethers, the experimental k_f values compare well with the anisoles, whereas those calculated from eq. [3] do not. This implies that the geometry of the adamantyl ethers changes on excitation from the 90° geometry in S_0 to the 0° geometry in S_1.

Fig. 5. X-ray crystal structure of **1h** (X = CF_3).

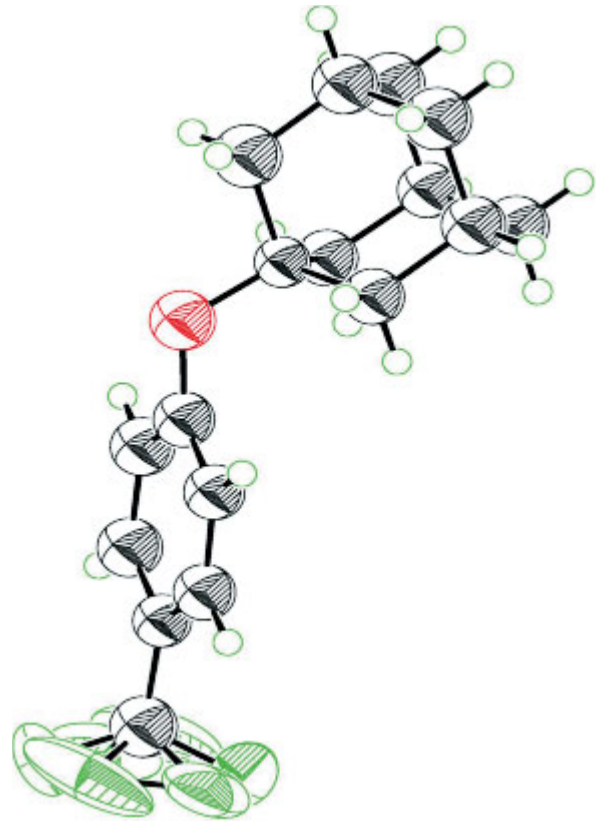

Fluorescence spectra of ethers 1 and 2

Values for the $\lambda_{0,0}$ (from the overlap of emission and excitation spectra), derived singlet state energies (E_{S1} (kJ/mol) = [1.197 × 10^5]/$\lambda_{0,0}$ (nm)), and fluorescence quantum yields for the anisoles **2** and adamantyl ethers **1** are reported in Table 1. Sample fluorescence spectra for the ethers **1** and **2** with X = H, 4-OCH_3, and 4-CN[4] are shown in Fig. 6, for both methanol (left in each case) and cyclohexane (right in each case). The spectra for the corresponding allyl ethers **4** are also included.

Two features are obvious from the spectra. The first is the very similar wavelength dependence unrelated to the structural change in the alkyl group (from adamantyl to methyl to allyl) in the ether. The only significant exception, a shift to a longer wavelength of about 5 nm for the adamantyl ether, occurs when X = 4-CN in Fig. 6, a case where intramolecular charge transfer in the excited state may be important. Other than this case, the spectra imply that the excited-state geometries of the ethers **1**, **2**, and **4** are similar. This suggestion is reinforced by the similar values of E_{S1} obtained for the anisoles and the adamantyl ethers.

Fig. 6. Fluorescence spectra of the ethers **1**, **2**, and **4** for X = H, 4-OCH_3, and 4-CN in methanol (left) and cyclohexane (right).

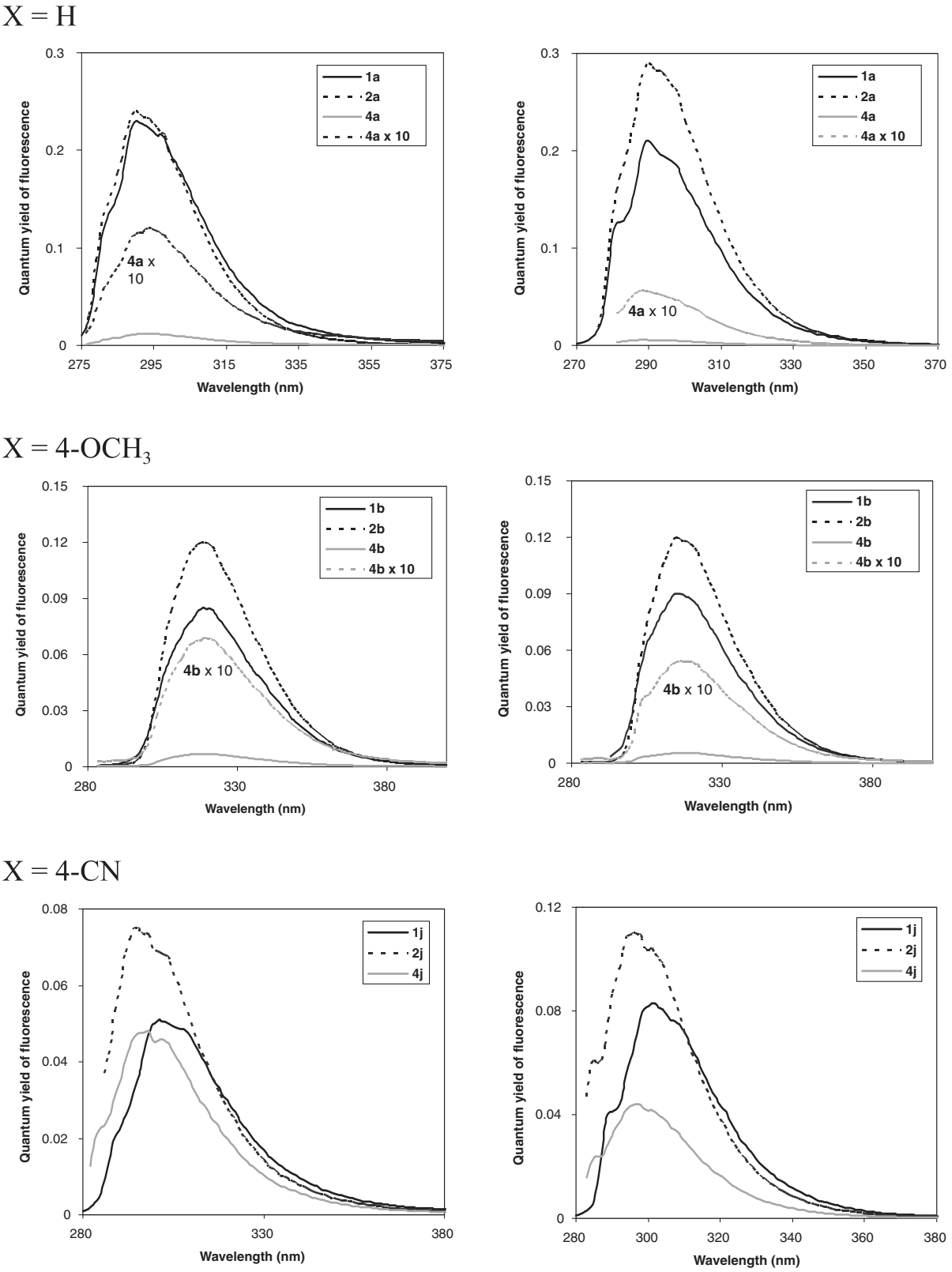

The second feature of these spectra is the difference in quantum yields of fluorescence. In general, the adamantyl ethers **1** and the anisoles **2** have similar Φ_fs in either solvent, the adamantyl ether values being somewhat lower. In contrast, the allyl ethers **4** have significantly lower Φ_f values than both **1** and **2**. These decreases for compounds **4** reflect the very large increases in reactivity of the excited singlet state relative to the anisoles **2**. As will be described in the

following, according to eq. [4], the higher values of k_r for the allyl ethers result in higher values of k_t, and, consequently, lower values for $\Phi_f = k_f/k_t$, k_f being essentially constant for any given substituent X but independent of the alkyl group of the ether. The similar values of Φ_f for the adamantyl ethers and the anisoles indicate that the k_r values for the adamantyl compounds do not make a large contribution to the k_t of S_1.

$$[4] \qquad k_t = k_f + k_{ic} + k_{isc} + k_r$$

Molecular orbital calculations

Excitation energies to S_1 were calculated by TDDFT/6-31G1(d) (20) using vertical excitations from the optimized ground-state geometries calculated previously for both the $\Phi = 0°$ and 90° conformer, again for the substituents shown in Table 2. In all cases, as expected, the calculated oscillator strength was lower for the 90° than the 0° conformer. Moreover, also in agreement with the UV absorption spectra, the excitation energy was higher for the $\Phi = 90°$ geometry than for the 0° geometry. Combined with the ground-state energies, the relative energies for the excited singlet state ($\Delta E(S_1)$) in Table 1 can be calculated indicating that, for all substitutents, S_1 for the 0° conformer is more stable than S_1 for the 90° conformer. This observation supports the suggestion that excitation of compounds **1** from S_0 at $\Phi = 90°$ gives S_1 at 90°, which then relaxes by rapid rotation to give the more stable conformer S_1 at 0°. Fluorescence emission and reaction should then occur from the 0° conformer.

Rate constants of reaction (k_r) from the excited singlet state of the adamantyl ethers 1

The quantum yield method, as described by eq. [1], for obtaining rate constants for excited-state bond cleavage reactions has a major defect. In all cases where experiments have been designed to detect it, internal return of radical pair intermediates (k_{ir} in Scheme 1) has been observed (1). Therefore, the efficiency of product formation that a quantum yield measures does not give a reliable measure of k_r. In effect, k_{ir} is a form of internal conversion, although not occurring directly from S_1. A knowledge of the fraction of this internal return [$k_{ir}/(k_p + k_{ir})$], which is undoubtably dependent on the substituent X, could be used to obtain correct values of k_r, but this fraction is a difficult number to obtain experimentally without a suitable probe. For instance, in the cases examined for the allyl ethers (**4a**–**4d**) in both methanol and cyclohexane, the importance of k_{ir} was demonstrated by the fact that the quantum yield method (eq. [1]) gave significantly lower values of k_r than the unreactive model method (eqs. [4] and [5]) (3), described in the following. With no suitable probe for the adamantyl ethers **1**, we decided not to measure quantum yields of reaction.

$$[5] \qquad k_t^M = k_f + k_{ic} + k_{isc}$$

The unreactive model method

For the allyl ethers **4**, we recently described an alternate method of measuring k_r for reactions of S_1 that relies on comparing a photochemically reactive compound with an unreactive one that has identical excited-state properties (3). We chose to compare compounds **4** with the anisoles **2**, which are, in comparison, photochemically inert. Either static (Φ_f) or dynamic (τ_s) measurements of fluorescence can be used although the latter is preferred because more reliable experimental values can be obtained. The assumption used is given in eqs. [4] and [5], where the changes in k_t of the reactive series only differ from those (k_t^M) of the model series **2** by k_r. Therefore, subtraction of experimentally determinable values ($k_t - k_t^M = k_r$) should reliably give k_r. Because these are exclusively properties of the excited singlet state, the k_r values obtained are independent of k_{ir}, the internal return process.

This method was applied quite successfully to obtain k_r values for the allyl ethers **4** in both cyclohexane and methanol (3). From absorbance spectra (λ_{max}, ϵ), fluorescence spectra ($\lambda_{0,0}$, E_{S1}), and calculated k_f values, good evidence was provided that the sets **2** and **4** have very similar excited-state properties for any given equivalently substituted pair in either methanol or cyclohexane. The resulting k_r values as a function of substituents spanned almost two orders of magnitude (10^8–10^{10} s^{-1}), and for some cases (3- and 4-methoxy and 3- and 4-methyl), were the dominant mode of decay of S_1. A plot of k_r in methanol vs. k_r in cyclohexane was linear and the slope (0.96) indicated a parallel substituent effect in the two solvents. This observation demonstrates that only radical pair intermediates are being generated, ion pairs not being possible in cyclohexane.

An examination of the k_t (adamantyl ethers **1**) and k_t^M (anisoles **2**) values in Table 1 indicates that the difference required to usefully apply eqs. [4] and [5] is hardly outside experimental error for most substitutents. Small positive values are obtained in most cases, although a few are actually negative. This observation quantitatively demonstrates that the adamantyl ethers have very small values of k_r, the rate constant of reaction, relative to the other modes of decay of the excited singlet state (k_{ic}, k_f, and k_{isc}). The only noticeable trend in the k_r values is towards higher values for those compounds **1j** and **1k** with cyano substitutents at C-3 and C-4, respectively, more so in methanol than in cyclohexane, but particularly for the 4-CN compound in methanol. This correctly accounts for the observation that the 4-cyano compound gives a significant yield of the ion-derived product **10** in methanol. Unfortunately, overall, the changes in k_r are too small to attempt a quantitative substituent effect correlation.

The temperature dependence of the fluorescence method

The effect of temperature on photochemical reactions has received far less attention than it deserves. However, recent studies from the laboratories of Lewis (activation barriers to E to Z isomerization in phenyl substituted alkenes) (25) and Zachariasse (thermally activated internal conversion in amino substitued aromatics) (26) have shown that the measurement of fluorescence quantum yields and lifetimes and intersystem crossing quantum yields over a wide temperature range provides a valuable tool to obtain rate constants for excited singlet state processes. Again, because the properties measured are exclusively those of S_1, the rate constants k_r obtained are independent of processes like k_{ir} or reaction from T_1. We have recently applied this approach to the phototransposition reactions of substituted benzenes (27).

The simplest assumption used is presented in eq. [6], which is the same as eq. [4] except that the reaction process k_r is considered to follow the Arrhenius expression. For

substituted benzenes, the S_0 to S_1 energy gap is large so that $k_{ic} \simeq 0$ ($k_{ic} \simeq 10^3$ s^{-1} for benzene with $E(S_1)$ = 444 kJ/mol).[7] Because $S_1 \rightarrow T_1$ is an exergonic process and considered to be unactivated, the rate of intersystem crossing should be temperature independent. However, Zachariasse and coworkers (26) have clearly shown that for amino substituted aromatics, $S_1 \rightarrow T_n$ intersystem crossing can be an important process that will be activated. Therefore, the total rate of intersystem crossing should be expressed by eq. [7], where k^0_{isc} is the intersystem crossing rate constant at 0 K (temperature independent), and the Arrhenius activation term is for the activated k_{isc}. The activation parameters for this process are characterized by low values of $A_{isc} \simeq 10^8$ to 10^9 s^{-1} and $E_{a/isc} \simeq$ 4–6 kJ/mol.

$$[6] \qquad k_t = k_f + k_{ic} + k_{isc} + A \exp(-E_a/RT)$$

$$[7] \qquad k_{isc} = k^0_{isc} + A_{isc} \exp(-E_{a/isc}/RT)$$

Values for k_t as a function of temperature have normally been obtained by measuring S_1 lifetimes (τ_s), but this is a very time-consuming process. We have chosen a more rapid method using τ_s and Φ_f at 25 °C (Table 1) to obtain $k_f = \Phi_f/\tau_s$. Then measurement of relative fluorescence quantum yields over a wide temperature range (–25 to 65 °C in methanol and –25 to 95 °C in methylcyclohexane)[8] were done (see Experimental section), and $k_t(T) = \Phi_f(T)/\Phi_f(25\ °C)$ values obtained assuming k_f is constant, independent of temperature. In fact, although k^0_f (the superscript refers to the refractive index (n) of vacuum) is temperature independent, the usual experimental observation for solution measurements is given in eq. [8] where the refractive index of the solvent is temperature dependent. However, over the temperature range studied here, the change in n^2 for the two solvents used is insignificant. From literature values[9] of the variation in refractive index with temperature (28), the k_f values for anisole would only change from 3.1×10^{-7} to 3.3×10^{-7} s^{-1} from –25 to +65 °C in methanol, and from 3.5×10^{-7} to 3.9×10^{-7} s^{-1} from –25 to 95 °C in methylcyclohexane. These ranges do not exceed the estimated error of 10% in k_f (assuming an error of 10% in Φ_f), and consequently, were ignored.

$$[8] \qquad k_f = k^0_f n^2$$

Plots of k_t vs. T are nonlinear and examples are shown in Fig. 7 for anisole, 4-cyanoanisole, and 4-cyanophenyl adamantyl ether (**1j**) in methanol. Other results are compiled in Table 3 for the adamantyl ethers **1** and the corresponding anisoles **2** for X = H, 4-OCH_3, and 4-CN.[4] Excellent fits of this data to eq. [6] were obtained ($r > 0.997$ in all cases) giving an intercept equal to $k_f + k_{isc}$ (assuming $k_{ic} = 0$) and Arrhenius A and E_a values. Using the independently determined experimental values of k_f gives k_{isc}. The consistency of the results is indicated by the similar values of k_{isc} obtained for any given pair of **1** and **2** with the same substituent and in either solvent.

Many of the compounds studied behave in a similar way to anisole in Fig. 7, with very little change in k_t as a function of temperature. As shown in Table 3, this results in low A values (2.6–8.6 × 10^9 s^{-1}) that are characteristic of an activated intersystem crossing process and indicate that the dominant temperature-dependent process for these substrates even at room temperature is k_{isc}, according to eq. [7]. This conclusion was also reached by a previous study on the temperature dependence of k_t (29), in 3-methylpentane and ethanol–methanol (1:1), although the A values (~2.5 × 10^8) reported are even lower than ours. The values of k_{isc} obtained by us for anisole at 25 °C of (10.0 ± 1.2) × 10^{-7} s^{-1} (methanol) and (9.1 ± 0.9) × 10^{-7} s^{-1} (methylcyclohexane) are in good agreement with literature values of 8.0 × 10^{-7} s^{-1} (cyclohexane) (30) and 9.4 × 10^{-7} s^{-1} (isooctane) (31), both obtained from directly measured Φ_{isc}/τ_s values. Moreover, the contribution that k_r makes to the total rate of decay of S_1 for anisole is small because $\Phi_f + \Phi_{isc}$ = 0.24 + 0.74 (29) (Ermolaev's rule) in agreement with the observation that irradiation of anisoles does not result in product formation. Very likely, the dialkoxy compounds **2**, with low A and E_a values, also have $\Phi_f + \Phi_{isc} \simeq 1$, and therefore they have $\Phi_{isc} \simeq$ 0.9 in both solvents, on the basis of $\Phi_f \simeq 0.1$ (Table 1).

As shown in Fig. 7, 4-cyanoanisole has a larger change in k_t as a function of temperature than does anisole even though both are photochemically unreactive in methanol. This suggests that both k_{isc} and k_r are contributing to the temperature dependence, but that the k_r process does not lead to products. As has been shown previously (26), to separate the activated k_{isc} and k_r rate constants reliably would require a combination of eqs. [6] and [7] and measurements over a much wider range of temperatures so that the process with lower A and E_a values (k_{isc}) would be dominant at low temperatures and k_r (higher A and E_a values) would be dominant at higher temperatures. Quantum yields of intersystem crossing as a function of temperature would also be required.

However, we have recently shown (27) that substituted aromatics undergo an activated process to form prefulvene biradicals. These intermediates (**18**–**20**), as in Scheme 3 for 4-methylbenzontrile (32), provide a pathway for both phototransposition reactions (ortho, meta, para) and also a pathway for k_{ir}, i.e., a chemical rather than photophysical route for internal conversion. We have also estimated (27) a quantum yield of Φ_r = 0.29 for the formation of **18**, and measured a quantum yield of formation of the meta isomer of Φ_p = 0.025 from the para one. Therefore, less than 10% of the intermediate **18** formed undergoes rearrangement to **19**. We suggest that formation of a prefulvene biradical is also the activated k_r process for 4-cyanoanisole. A similar activated internal conversion has been observed (26) for 4-cyanoaniline (and other aromatic amines in hydrocarbon solvents) with E_a = 35 kJ/mol and $A \simeq 5 \times 10^{12}$ s^{-1}. The authors noted that an activated, but undefined, geometric deformation in S_1 must be providing a pathway for S_1 to S_0 decay.

If this proposal is correct, then the difference in k_r between the anisoles and the adamantyl ethers obtained from the variable temperature studies reflects the increased reactivity of the adamantyl ethers because of C—O bond cleavage. This suggestion assumes that the activated k_{isc} and the

[7] See, in particular, the Introduction section of ref. 26.

[8] For the variable temperature studies, methylcyclohexane, rather than cyclohexane, was used as the solvent to expand the range of experimentally accessible temperatures.

[9] This reference gives values of dn/dt = –0.000 39/°C for methanol and –0.000 55/°C for cyclohexane.

Fig. 7. Temperature dependence of k_t and the fits to eq. [6] for the compounds **1j** (X = 4-N), **2j** (X = 4-CN), and **2a** (X = H) in methanol.

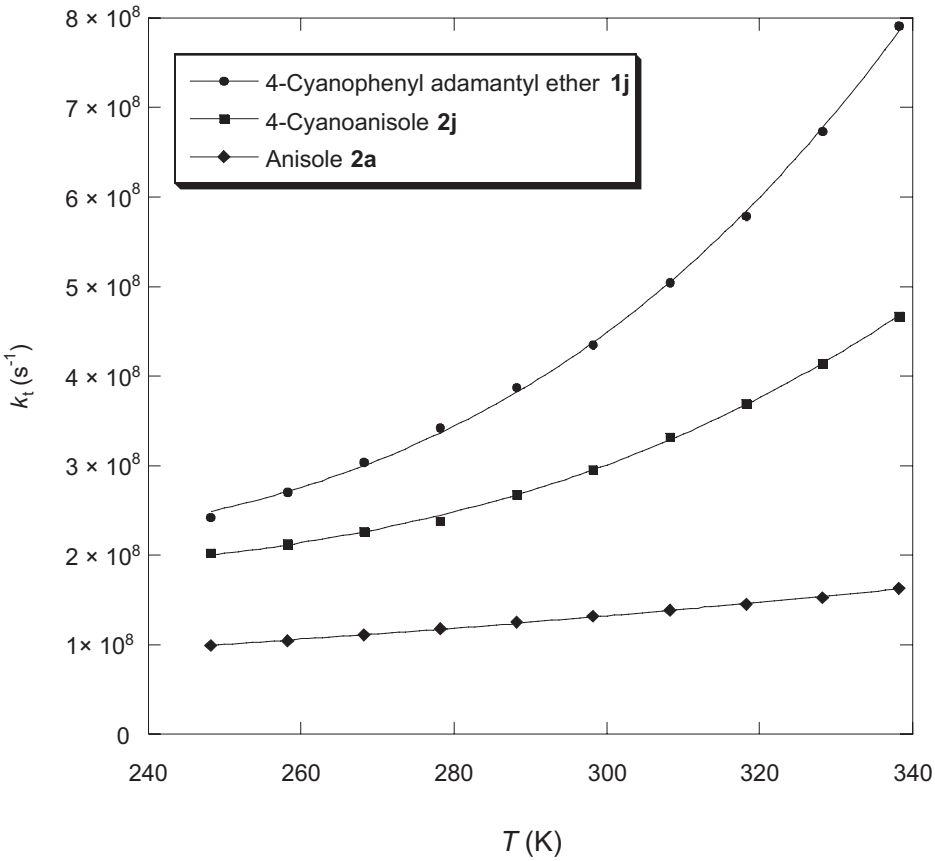

4-Cyanophenyl adamantyl ether

y = m1+m2*exp(-m3/(8.314e-3*T))		
	Value	Error
m1	1.9576e+08	8.318e+06
m2	4.4908e+11	1.0285e+11
m3	18.657	0.66811
Chisq	2.107e+14	NA
R	0.99965	NA

4-Cyanoanisole

y = m1+m2*exp(-m3/(8.314e-3*T))		
	Value	Error
m1	1.7267e+08	4.6846e+06
m2	2.0355e+11	5.105e+10
m3	18.377	0.73277
Chisq	6.3681e+13	NA
R	0.99957	NA

Anisole

y = m1+m2*exp(-m3/(8.314e-3*T))		
	Value	Error
m1	6.8121e+07	6.2294e+06
m2	1.8841e+09	4.9421e+08
m3	8.4225	0.90553
Chisq	6.8794e+12	NA
R	0.99914	NA

other k_r processes (for instance, formation of the prefulvene biradical) are similar in rate for the equivalently substituted adamantyl ether and anisole. The difference in the temperature dependence between 4-cyanoanisole (**2j**) and adamantyl 4-cyanophenyl ether (**1j**) is clearly shown in Fig. 7, and the values of Δk_r (25 °C) in the last column of Table 2 support this suggestion. The values are larger in methanol than methylcyclohexane for all substrates studied, in agreement with the observation that the efficiency of photochemical conversion of the adamantyl ethers is greater in methanol. Moreover, both the substituted adamantyl ethers (4-OCH_3, 4-CN) react faster than the unsubstituted one. Most notable is the high k_r value for the 4-CN substrate in methanol, presumably as a result of the k_r process leading to ion pairs from S_1 and the resulting product 1-methoxyadamantane.

Conclusions

A variety of techniques have demonstrated that the adamantyl ethers **1** have a ground-state geometry with a dihedral angle of 90° that reduces conjugation of the ether oxygen with the aryl ring. Upon excitation to S_1, the geometry relaxes to a 0° conformer that increases the conjugation but decreases the overlap between the aromatic π system and the bond that breaks in the excited state. This observation provides an explanation for the low photochemical reactivity of these ethers and the lack of any large substituent effect on the rate constant of bond cleavage from S_1. For substrates that do not react, this technique provides a simple method of determining k_{isc} and Φ_{isc}. The method also allows a comparison between unreactive model compounds (the anisoles) and reactive substrates (the adamantyl ethers) so that the k_r process that leads to products or reactive intermediates can be separated from that which leads back to starting material (k_{ir}), a form of internal conversion.

Experimental

General procedures

Routine ^{1}H and ^{13}C NMR spectra were obtained in $CDCl_3$ on a Bruker AC 250 F NMR spectrometer in automation mode. The ^{13}C NMR spectra for **1a**–**1j** in Table S1 (Sup-

Table 3. Fits to eq. [6] and derived rate constants for S_1 of adamantyl ethers **1** and anisoles **2**.

	X	Solvent[a]	A^b ($10^9 s^{-1}$)	$E_a{}^b$ (kJ/mol)	$k_f + k_{isc}{}^c$ ($10^7 s^{-1}$)	$k_f{}^d$ ($10^7 s^{-1}$)	$k_{isc}{}^e$ ($10^7 s^{-1}$)	$k_t{}^f$ ($10^7 s^{-1}$)	$k_r{}^g$ ($10^7 s^{-1}$)	$\Delta k_r{}^h$ ($10^7 s^{-1}$)
1a	H	M	3.0 (1.3)	9.2 (1.4)	8.7 (1.0)	3.7 (0.4)	5.0 (1.4)	16.1 (0.2)	7.4 (1.2)	1.0 (1.5)
2a	H	M	1.8 (0.4)	8.4 (0.9)	6.8 (0.2)	3.2 (0.3)	3.6 (0.9)	13.2 (0.1)	6.4 (0.3)	
1a	H	MC	24 (1.0)	16.0 (1.0)	10.6 (0.4)	3.0 (0.3)	7.6 (0.7)	14.3 (0.1)	3.7 (0.5)	0.2 (0.8)
2a	H	MC	3.8 (0.6)	11.6 (0.6)	9.3 (0.2)	3.7 (0.4)	5.6 (0.6)	12.8 (0.1)	3.5 (0.3)	
1b	4-OCH_3	M	4.9 (0.3)	7.7 (0.2)	17.7 (0.1)	3.4 (0.3)	14.3 (0.4)	40.0 (0.4)	25.7 (0.8)	8.9 (1.3)
2b	4-OCH_3	M	3.6 (0.5)	7.6 (0.6)	20.5 (0.1)	4.1 (0.4)	16.4 (0.5)	37.3 (0.4)	16.8 (0.5)	
1b	4-OCH_3	MC	4.4 (0.4)	8.5 (0.4)	17.4 (0.1)	2.6 (0.3)	14.8 (0.4)	32.0 (0.3)	14.6 (0.4)	4.9 (0.9)
2b	4-OCH_3	MC	8.6 (0.6)	10.7 (0.2)	21.6 (0.3)	4.0 (0.4)	17.6 (0.6)	31.3 (0.3)	9.7 (0.5)	
1j	4-CN	M	450 (10)	18.7 (0.7)	19.6 (0.1)	2.2 (0.2)	17.4 (0.3)	43.5 (0.4)	23.9 (0.5)	11.6 (1.3)
2j	4-CN	M	200 (50)	18.4 (0.7)	17.3 (0.5)	2.2 (0.2)	15.1 (0.7)	29.6 (0.3)	12.3 (0.8)	
1j	4-CN	MC	240 (7)	21.0 (1.0)	17.3 (0.4)	1.9 (0.2)	15.4 (0.6)	22.6 (0.2)	4.3 (0.6)	0.3 (1.1)
2j	4-CN	MC	12.3 (6)	14.1 (0.9)	13.0 (0.3)	1.9 (0.2)	11.1 (0.5)	17.0 (0.2)	4.0 (0.5)	

Note: Values in brackets are estimated errors: from fits to eq. [6] for A, E_a, and $(k_f + k_{isc})$; from ±10% for ϕ_f; from ±1% for τ_s; from accumulated errors for calculated quantities.

[a]Solvent: M (methanol), MC (methylcyclohexane).
[b]Arrhenius parameters from eq. [6].
[c]Intercept from eq. [6].
[d]$k_f = \phi_f k_t$.
[e]$(k_f + k_{isc}) - k_f$.
[f]$k_t = 1/\tau_s$ from nanosecond single photon counting at 25 °C.
[g]$k_r(25\ °C) = k_t(25\ °C) - (k_f + k_{isc})$.
[h]$k_r(\mathbf{1}) - k_r(\mathbf{2})$ at 25 °C.

Scheme 3. Mechanism for the phototransposition of *para*-methylbenzonitrile to the meta and ortho isomers and associated rate constants of reaction.

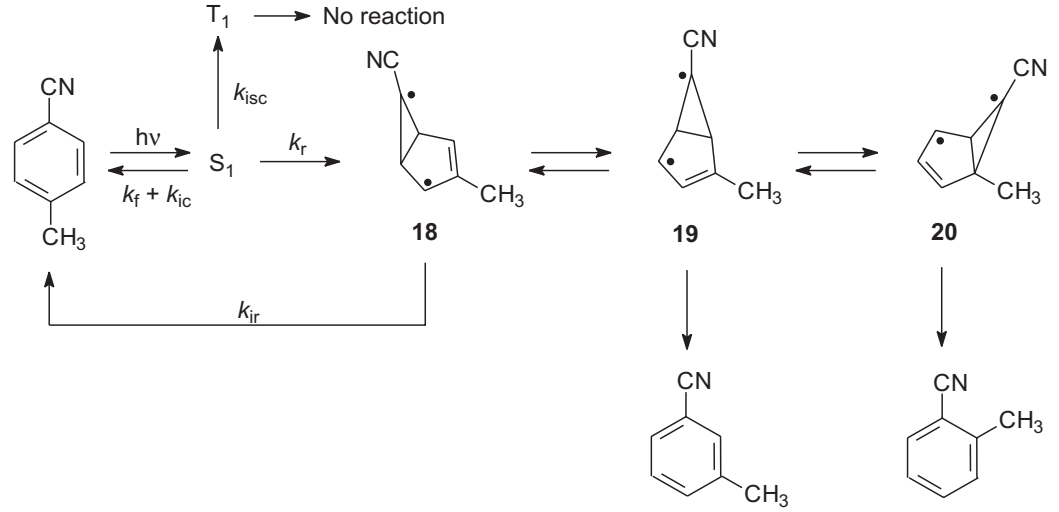

porting information)[3] were obtained on a Bruker AVANCE 500 MHz spectrometer with chemical shifts (δ) reported relative to the central line of $CDCl_3$ at 77.16 ppm. GC–MS analyses were performed on a PerkinElmer Autosystem XL instrument with a mass selective detector. The column used was a Supelco 30 m × 0.25 mm MDN-5S 5% phenyl methylsiloxane, film thickness 0.50 µm; temperature program: 60 °C for 1 min; 20 °C/min to 240 °C; 240 °C for 10 min. GC-FID analyses were done in a similar way except on a Supelco DB200 column. Mass spectral data are reported in units of mass over charge (*m*/*z*) for all values between 50 and the molecular ion if greater than 10% of the base peak. Intensities are reported as a percent of the base peak. HR-MS were obtained on a CEC 21-110 instrument with a resolution of 5–10 × 10^3. The solvents used for photochemical reactions and fluorescence measurements were used as received: methanol (EM, HPLC), cyclohexane (Aldrich, HPLC), and methylcyclohexane (Aldrich, spectrophotometric grade).

Preparation of the adamantyl aryl ethers 1a–1k

The ethers were synthesized by a modified literature method (9) from 1-bromoadamantane and the substituted phenol (Aldrich). In a typical procedure, a mixture of 8.40 g (75 mmol) of 4-fluorophenol and 3.24 g (15 mmol) of 1-bromoadamantane and 4.5 mL of pyridine was refluxed for 5 h. The reaction mixture was cooled, diluted with 50 mL of water – ethylene glycol (8:1), and extracted with 2 × 15 mL

of hexanes. The extract was washed with 5% NaOH (25 mL), water (2 × 25 mL), dried ($MgSO_4$), and the hexanes evaporated. The crude solid (2.26 g) was purified by flash chromatography using 2.5% ethyl acetate in hexanes to give 1.14 g (31%) of a colourless solid that was recrystallized from methanol.

Characterization of the adamantyl aryl ethers 1a–1k

^{1}H NMR spectra were not particularly diagnostic: the signals expected for the substituted benzene ring, the substituent for X = OCH_3 and CH_3, and the 1-adamantyl ring system (δ 2.17, 1.89, and 1.61, all broad singlets) were all present. ^{13}C NMR spectral data for the ethers **1**, along with those for **2**–**4** are reported in Table S1 (Supporting information).[3] Mass spectral data (GC–MS) were also not particularly diagnostic: a molecular ion (but not for X = 3-CF_3, 4-CF_3, 3-CN, and 4-CN) and $C_{10}H_{15}$, the adamantyl cation as the base peak (100) and its fragment ions at 107 (12), 93 (22), 79 (25), and 77 (13) were observed. Other characterization results: **1a** (X = H): mp 112 to 113 °C (lit. value (33) mp 99 to 100 °C). **1b** (X = 4-OCH_3): mp 48 to 49 °C (lit. value (33) mp 49–51 °C). **1c** (X = 3-OCH_3): mp 44–46 °C. HR-MS calcd. for $C_{17}H_{22}O_2$: 258.1620; found: 258.1628. **1d** (X = 4-CH_3): mp 53.5–54.0 °C (lit. value (33) mp 41–43 °C). **1e** (X = 3-CH_3): mp 69.0–70.0 °C. HR-MS calcd. for $C_{17}H_{22}O$: 246.1671; found: 246.1668. **1f** (X = 4-F): mp 110 to 111 °C. HR-MS calcd. for $C_{16}H_{19}OF$: 246.1420; found: 246.1423. **1g** (X = 3-F): mp 38 to 39 °C. HR-MS calcd. for $C_{16}H_{19}OF$: 246.1420; found: 246.1419. **1h** (X = 4-CF_3): mp 57.5–58.5 °C. **1j** (X = 4-CN): characterized previously (2). **1k** (X = 3-CN): mp 86 to 87 °C.

Irradiation of ethers

A solution of ~100 mg of the appropriate ether in 100 mL of methanol or cyclohexane was purged with nitrogen and then irradiated in a Rayonet photochemical reactor using 16 lamps (75 W, 254 nm). The temperature was kept at 25 °C by circulating water in an immersion tube. Reaction progress was monitored by GC.

Absorbance measurements

Absorbance spectra were recorded at 1 nm resolution using a Cary 100 UV–vis spectrometer thermostatted at 25 °C. Selected examples are shown in Fig. 1. The integrated spectra needed to obtain k_f values from eq. [3] were obtained by summing the 1 nm incremental areas (the absorbance values converted to ϵ by dividing by the molar concentration) over the complete absorption band. These areas are somewhat uncertain at the short wavelength end because of overlap with the long wavelength tail of the S_2 band so that the absorbance does not reach zero. The wavelength for the minimum in absorbance was used as the cut-off point for the S_1 band. For the 4-cyano and 4-trifluoromethyl derivatives of **1** and **2**, this overlap was too extensive to allow integration of the S_1 band and k_f values were not calculated.

Fluorescence measurements

All samples were degassed by three freeze–pump–thaw cycles and then thermostatted at 25 °C. The substituted anisoles used for comparison were all commercial samples (Aldrich) and were distilled before use. Fluorescence intensity measurements were done using a PTI-210M fluorescence spectrometer with dual model 101 monochromators, a 75 W Xenon lamp, and a model 814 photomultiplier detector. Corrected spectra were obtained. Selected examples are shown in Fig. 6. Fluorescence quantum yields were determined using solutions of matched absorbance by comparison with the known fluorescence quantum yield of 0.24 (30) for anisole in methanol and 0.29 (34) in cyclohexane. The expectation values necessary for calculating the k_f values from eq. [3] were obtained by summing the 1 nm incremental areas over the complete emission band. For temperature-dependent quantum yield measurements, a 1 cm cuvette was thermostatted with stirring in a cuvette holder equipped with a Quantum Northwest TLC 50 temperature controller, which allows relative fluorescence measurements at 10 °C intervals from –25 to 95 °C in methylcyclohexane and –25 to 60 °C in methanol over a 2 h time span. The stability of the lamp over this time period was normally confirmed by rerunning the fluorescence spectrum at 25 °C at the end.

Singlet lifetimes were measured at 25 °C by monitoring fluorescence decay using a PRA time-correlated, single-photon-counting apparatus with a hydrogen flash lamp of with a pulse width of about 1.8 ns.

Acknowledgments

We thank the Natural Sciences and Engineering Research Council of Canada (NSERC) for financial support, Sepracor Canada Ltd., Windsor, Nova Scotia for the donation of chemicals, and Lei Zhang, Department of Chemistry and Biochemistry, Concordia University, Montreal, for assistance with the Gaussian calculations.

References

1. S.A. Fleming and J.A. Pincock. Organic molecular photochemistry. Vol. 3. Marcel Dekker, New York. 1999. p. 211.
2. D.P. DeCosta, A. Bennett, A.L. Pincock, J.A. Pincock, and R. Stefanova. J. Org. Chem. **65**, 4162 (2000).
3. A.L. Pincock, J.A. Pincock, and R. Stefanova. J. Am. Chem. Soc. **124**, 9768 (2002).
4. J. McEwen and K. Yates. J. Phys. Org. Chem. **4**, 193 (1991).
5. E.L. Wehry and L.B. Rogers. J. Am. Chem. Soc. **87**, 4234 (1965).
6. P.J. Baldry. J. Chem. Soc. 951 (1979).
7. (*a*) S.C. Shim, J.W. Park, and H.-S. Ham. Bull. Korean Chem. Soc. **3**, 13 (1982); (*b*) S.C. Shim, J.W. Park, H.-S. Ham, and J.-S. Chung. Bull. Korean Chem. Soc. **4**, 45 (1983).
8. T.F. Wolwode, C. Rose, and T.J. Wandless. J. Org. Chem. **63**, 9594 (1998).
9. H. Masada and Y. Oishi. Chem. Lett. 57 (1978).
10. J. Bartl, H. Mayr, and R.A. McClelland. J. Am. Chem. Soc. **112**, 6918 (1990).
11. H.E. Zimmerman and S. Somasekhara. J. Am. Chem. Soc. **85**, 922 (1963).
12. Y.-R. Luo. Handbook of bond dissociation energies in organic compounds. CRC Press, Boca Raton, Fla. 2003.
13. D.C. Spellmeyer, P.D.J. Grootenhuis, M.D. Miller, L.F. Kuyper, and P.A. Kollman. J. Phys. Chem. **94**, 4491 (1990).
14. (*a*) T. Schaefer and G.H. Penner. Can. J. Chem. **66**, 1635 (1988); (*b*) T. Schaefer and G.H. Penner. Can. J. Chem. **66**,

1641 (1988); (*c*) T. Schaefer and R. Sebastian. Can. J. Chem. **67**, 1148 (1989).
15. E. Taskinen. J. Chem. Soc. Perkin Trans. 2, 1824 (2001).
16. J.C. Dearden and W.F. Forbes. Can. J. Chem. **37**, 1305 (1959).
17. C.J. Pouchert and J. Behnke. The Aldrich library of ^{13}C and ^{1}H NMR spectra. Vol. 2. Aldrich Chemical Company, Milwaukee, Wis. 1993. pp. 175–241.
18. J. Bromilow, R.T.C. Brownlee, D.J. Craik, M. Sadek and R.W. Taft. J. Org. Chem. **45**, 2429 (1980).
19. K.S. Dhami and J.B. Stothers. Can. J. Chem. **44**, 2855 (1966).
20. M.J. Frisch, G.W. Trucks, H.B. Schlegel, G.E. Scuseria, M.A. Robb, J.R. Cheeseman, V.G. Zakrzewski, J.A. Montgomery, Jr., R.E. Stratmann, J.C. Burant, S. Dapprich, J.M. Millam, A.D. Daniels, K.N. Kudin, M.C. Strain, O. Farkas, J. Tomasi, V. Barone, M. Cossi, R. Cammi, B. Mennucci, C. Pomelli, C. Adamo, S. Clifford, J. Ochterski, G.A. Petersson, P.Y. Ayala, Q. Cui, K. Morokuma, N. Rega, P. Salvador, J.J. Dannenberg, D.K. Malick, A.D. Rabuck, K. Raghavachari, J.B. Foresman, J. Cioslowski, J.V. Ortiz, A.G. Baboul, B.B. Stefanov, G. Liu, A. Liashenko, P. Piskorz, I. Komaromi, R. Gomperts, R.L. Martin, D.J. Fox, T. Keith, M.A. Al-Laham, C.Y. Peng, A. Nanayakkara, M. Challacombe, P.M.W. Gill, B. Johnson, W. Chen, M.W. Wong, J.L. Andres, C. Gonzalez, M. Head-Gordon, E.S. Replogle, and J.A. Pople. GAUSSIAN 98. Revision A.11.2 [computer program]. Gaussian Inc., Pittsburgh, Penn. 2001.
21. B. Uno, T. Iwamoto, and N. Okumura. J. Org. Chem. **63**, 9794 (1998).
22. S.J. Strickler and R.A. Berg. J. Chem. Phys. **37**, 814 (1962).
23. J.B. Birks and D.J. Dyson. Proc. R. Soc. London Ser. A, **275**, 135 (1963).
24. R.B. Cundall and L.C. Pereira. J. Chem. Soc. Faraday Trans. **68**, 1152 (1972).
25. F.D. Lewis and X. Zuo. Spectrum (Bowling Green, OH, U.S.), **16**, 8 (2003). Available from www.bgsu.edu/departments/photochem/research/summer2003/spectrum.html.
26. S.I. Druzhinin, A. Demeter, V.A. Galievsky, T. Yoshihara, and K.A. Zachariasse. J. Phys. Chem. **107**, 8075 (2003), and refs. cited therein.
27. C.M. Gonzalez and J.A. Pincock. J. Am. Chem. Soc. **126**, 8870 (2004).
28. J. Timmermans. Physico-chemical constants of pure organic liquids. Vol. 1. Elsevier, New York. 1950.
29. S. Dellonte and G. Marconi. J. Photochem. **30**, 37 (1985).
30. G. Kohler, G. Kittel, and N. Getoff. J. Photochem. **18**, 19 (1982).
31. F.A. Carroll and F.H. Quina. J. Am. Chem. Soc. **94**, 6246 (1972).
32. (*a*) J.A. Pincock. *In* CRC handbook of organic photochemistry and photobiology. 2nd ed. *Edited by* W. Horspool and F. Lenci. CRC Press, Boca Raton, Fla. 2003. pp. 46–1 to 46–19; (*b*) P.J. MacLeod, A.L. Pincock, J.A. Pincock, and K.A. Thompson. J. Am. Chem. Soc. **120**, 13 354 (1998).
33. U. Kraatz. Chem. Ber. **106**, 3095 (1973).
34. I.B. Berlman. Handbook of fluorescence spectra of aromatic molecules. Academic Press, New York. 1971. p. 139.